POLAR MICRO-REGIONS AND SUPERLATTICE IN 7.9/70/30 PLZT CERAMICS

SONG XIANG-YUN (宋祥云), WEN SHU-LIN (温树林) AND YIN ZHI-WEN (殷之文)
(*Shanghai Institute of Ceramics, Academia Sinica, Shanghai* 200050, *PRC*)

Received May 28, 1989.

ABSTRACT

The microstructures of 7.9/70/30 $(Pb_{92.1}La_{7.9})(Zr_{70}Ti_{30})O_3$ (PLZT) transparent ferroelectric ceramics are studied by using the high-resolution electron microscopy (HREM) techniques and electron diffraction. The results indicate that the structure of micro-domains presented in the cubic α-phase is exactly the same as that of its ferroelectric β-phase after poling. The fringe-shape micro-regions, appearing in the HREM microphotograph of 7.9/70/30 PLZT, are the result from lattice-overlapping of the orthorhombic micro-domains and the cubic α-phase matrix. Furthermore, a $2\times d_{111}$ superlattice along the $\langle 111\rangle$-direction has been observed in 7.9/70/30 PLZT ceramics. This is probably the result of gliding or rotation on the (111)-plane of self-structure regulation due to point defects.

Key words: ferroelectric, polar micro-region, Moire, electron diffraction, superlattice.

Since the fringe-shaped micro-regions at 100 ~ 300 Å were observed under transmission electron microscopy (TEM) in α-phase of PLZT transparent ceramics[1], the micro-domain model[2] has helped to explain the phase transition behavior and the properities of relaxor ferroelectrics. However, whether these micro-regions are micro-domains and what is the correlation between these micro-regions and their micro-domains still need verifying. In recent years a superlattice structure of $2 \times d_{111}$ along the $\langle 111\rangle$-direction in 7.9/70/30 PLZT ceramics has been observed which also requires interpretation.

I. EXPERIMENTAL EVIDENCE AND DISCUSSION

As in the previous work, the synthesized 7.9/70/30 PLZT powder was prepared by means of alcohol dehydration of mixed citrate solutions[3]. After being cold pressed into cylindrical slugs with $\phi = 20$ mm and 20 mm in hight, the powder was hot pressed at oxygen atmosphere. For the TEM study, the samples were first ground and then polished into small disks with $\phi = 3$ mm and 20 μm in thickness, followed by thinning with an Ar-ion beam. The samples were observed under a JEOL-200CX transmission electron microscope. The experimental results will be discussed in the following two aspects.

1. *Polar Micro-Regions*

Fig. 1 is a microphotograph of the inhomogeneous distributed micro-regions ob-

served under HREM in PLZT grain of the α-phase. It can be seen that micro-regions are fringe-shaped with 50—300 Å dimension. The micro-regions in a single grain are similarly orientated, with fringe spacing D being 5—11 Å and more than half of them being 10 Å. According to the electron microscopical theory[4], the appearance of such micro-regions is probably the result of lattice-overlapping of two different symmetrical lattices, i.e. the Moire fringes.

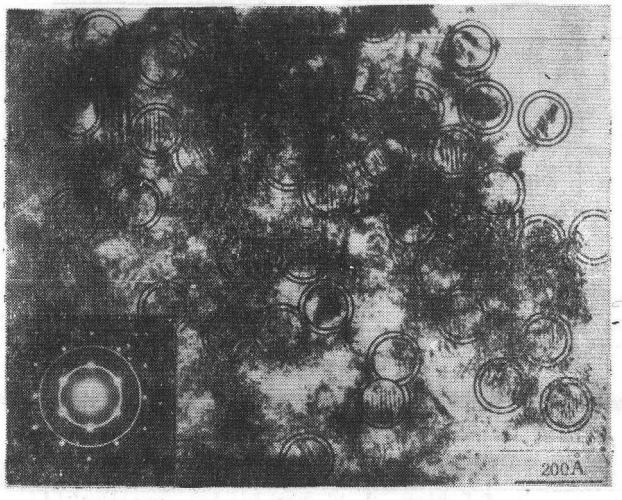

Fig. 1. HREM microphotograph of the PLZT sample showing the existence of fringe-shaped micro-regions in the α-phase (corresponding electron diffraction pattern on the lower left).

An electron diffraction pattern taken from the area possessing more micro-regions is shown in the lower left part of Fig. 1. This electron diffraction pattern can be divided into two portions. One portion is composed of spots arranged regularly in hexagon, which have been verified by electron diffraction indexing to be PLZT cubic α-phase along the $\langle 111 \rangle$-direction. The other portion is composed of diffraction disks with different intensities and individual stray spots. These diffraction disks and spots do not coincide with the diffraction spots of cubic [111], and even the innermost disk with high intensity does not coincide well with the cubic (110) diffraction spots either. It is difficult to use the lattice parameters of the cubic α-phase to perform indexing for these extra disks and spots, which implies that they are not contributed by the cubic α-phase structure. However, when the parameters of the orthorhombic β-phase ($a'=5.79$ Å, $b'=5.81$ Å, $c'=4.09$ Å)[5,6] of 7.9/70/30 PLZT are used to conduct indexing for these extra disks and spots, the results coincide with β-phase very well.

Fig. 2 shows the electron diffraction pattern taken from the same area of the same sample but along the $\langle 001 \rangle$-direction. Besides the spots regularly arranged in squares which belong to the cubic α-phase along $\langle 001 \rangle$, there are also individual stray spots, that can be indexed with structural parameters of the orthorhombic β-phase. Table 1 lists the results of indexing for these extra disks and spots in Figs. 1 and 2, in comparison with the corresponding values of the orthorhombic β-phase sample obtained from the X-ray diffraction data. Table 1 indicates that these[1] results

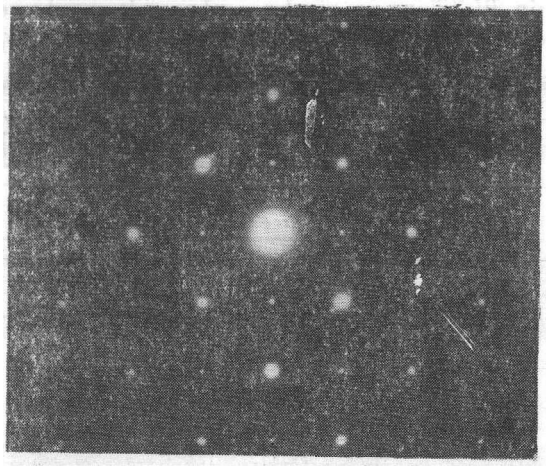

Fig. 2. Electron diffraction pattern taken from the same area of the PLZT sample as that in Fig. 1, but along the [001]-direction.

Table 1

Comparison of Result of Indexing for Extra Disks and Spots in Figs. 1 and 2 With Corresponding Values of Orthorhombic Phase Sample Derived From X-Ray Diffraction Data

Lattice Indexing	d_{111} (Å)	d_{210} (Å)	d_{310} (Å)	d_{311} (Å)
Orthorhombic β-phase in Fig. 1	2.89	2.59	1.84	1.67
Orthorhombic β-phase in Fig. 2	2.89		1.83	
Orthorhombic β-phase sample	2.896	2.591	1.832	1.67

Table 2

Result of Lattice-Overlapping of (111)-Planes of Orthorhomic Micro-Domains on (110)-Plane of Cubic-Phase Matrix

Fringe Sequence	d_1	d_2	d_3	d_4	d_5	d_6	d_7	d_8	d_9	d_{10}
Moire fringe space (Å)	7.7	10.4	8.7	10.1	10.0	9.2	2.6	5.5	6.2	11.0

are essentially identical.

Wei Zong-yin et al. worked on the diffraction intensity of different planes of the orthorhombic β-phase structure using the X-ray diffraction and showed that the (111)- and (311)-planes possess higher diffraction intensities. It is easy to see from Figs. 1 and 2 that those extra disks and spots with higher intensity are diffracted from the (111)- and (311)-planes.

In order to reveal in detail the information from the photograph using the structural parameters of the orthorhombic β-phase, we calculated the fringe spacing of the micro-regions in Fig. 1[4] with the results listed in Table 2. The result obtained shows that the fringe-shape micro-regions appearing in the HREM microphotograph

was caused by the lattice-overlapping of the (111)-planes of orthorhombic micro-domains on the (110)-plane of the cubic α-phase matrix. Table 2 manifests that most of the Moire fringe space are 5—11 Å, which is in agreement with the fringe image in Fig. 1 (5—11 Å). It also shows that the orthorhombic micro-domains exist in a magnitude of the order 100 Å (equivalent to 20—30 unit cells) in the cubic α-phase.

2. *Superlattice*

A superlattice structure along the ⟨111⟩-direction in $Pb(Zr_{09}Ti_{01})O_3$ ferroelectric ceramics has been reported by Michel et al.[7] Recently, we also discovered a similar superlattice in 7.9/70/30 PLZT. Figs. 3(a) and 3(b) show respectively the micro-morphology of a grain in 7.9/70/30 PLZT and its corresponding selected area electron diffraction (SAED) pattern taken from the dark area. Fig. 3(a) indicates that the ~7 μm grain in the center of the picture links up closely with the neighbouring grains as usual, but an area with a dark background in the center of the grain reveals the changes in the micro-srtucture of this area. The indexing indicates that the electron diffraction photograph (Fig. 3(b)) is the diffraction pattern of the cubic α-phase along the ⟨110⟩-direction. However, we can easily see from Fig. 3(b) that there are extra spots with lower intensity at the sites just in the middle between the transmission spots (000) and the (111)-diffraction spots. That implies the existence of planes along the ⟨111⟩-direction of this structure and its d-spacing is just twice that of the (111)-planes, i.e. $d = 2 \times d_{111} = 4.7$ Å.

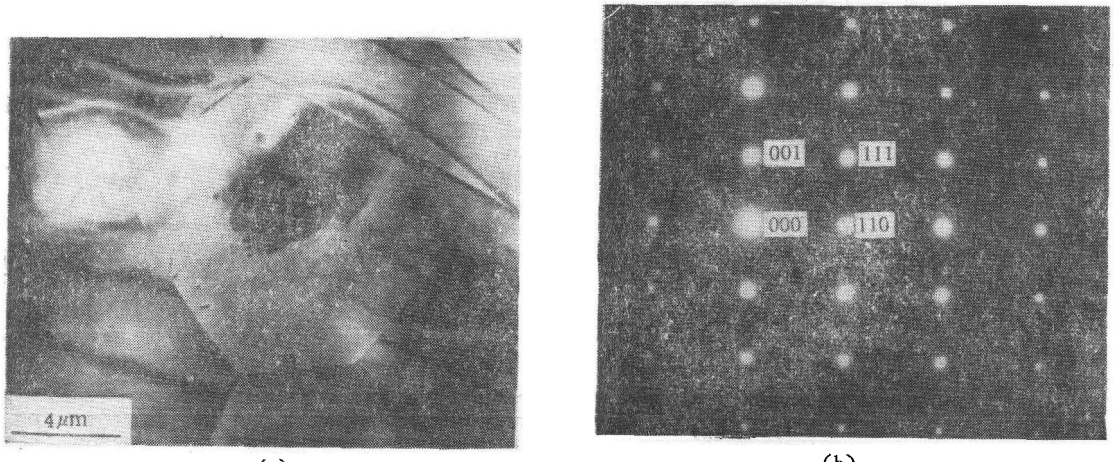

(a) (b)

Fig. 3. (a) Micro-morphology of a grain in PLZT grain; (b) selected area electron diffraction (SAED) pattern taken from the dark area in (a).

Now let us review the cubic α-phase of PLZT structure (Fig. 4(a)). Pb^{2+} or La^{3+} ions are located at the eight vertexes of the ABO_3 perorskite, and the Zr^{4+} or Ti^{4+} at the body-centred sites. Six O^{2-} ions are distributed on the face-centred sites, forming the octahedron structure with Zr^{4+} (or Ti^{4+}) ion. All the eight (111) planes of the Zr^{4+}(or Ti^{4+})O^{2-} octahedron are perpendicular to the ⟨111⟩-axis. Because the quantity of replacement of Pb^{2+} by La^{3+} is rather large (about 8 atomic percentage), there must be, for the need of electric balance, a certain amount of point vacancies in the structure, most of them being A-vacancies[8]. The formation and move-

ment of these point vacancies would give rise to corresponding regulations of other ions in the structure. These regulations occur on the (111)-planes because they are atomic close-packed in the cubic structure, and gliding or rotating occur readily on these planes. From Fig. 4(a) we can see that the projection from the [110]-direction should be that as shown in Fig. 5(a) during the absence of displacement of atoms.

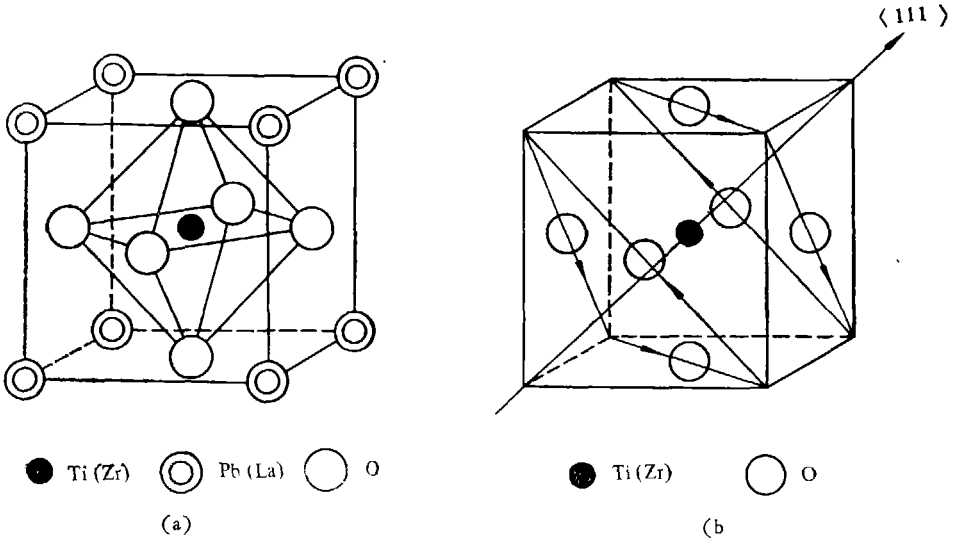

Fig. 4. (a) Perovskite structure of cubic PLZT; (b) superlattice $2\times d_{111}$ formed in PLZT following the plane rotation.

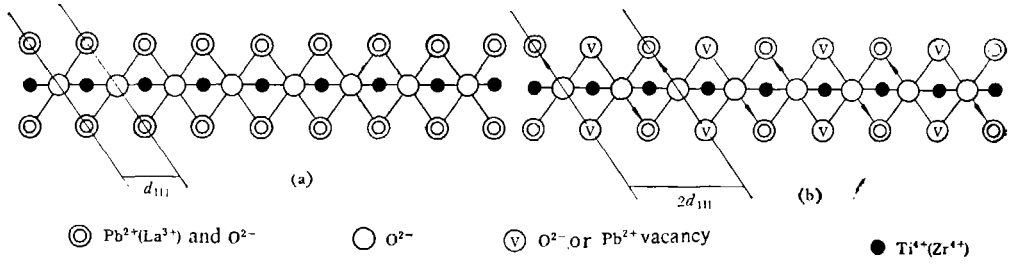

Fig. 5. (a) The [110] projection corresponding to Fig. 4(a); (b) the [110] projection corresponding to Fig. 4(b).

However, the oxygen atoms on the (111)-planes would be regulated correspondingly when La^{3+} or vacancy regularly appears at the La^{3+} or Pb^{2+} site. According to the diffraction result (Fig. 3(b)), we assume that when two neighbouring (111)-planes (oxygen atomic plane) in Fig. 4(b) rotate around the ⟨111⟩-axis in opposite directions by a certain angles, a superlattice along the ⟨111⟩-direction forms and its plane spacing twice that of (111)-planes might occur (see Fig. 5(b)). Song Xiang-yun et al.[9] investigated the lattice energy of PLZTs at different Zr/Ti ratios and found that as the Zr content in PLZT increased, the stability of PLZT lattice decreased. So, different defects as well as superlattice will easily occur in PLZTs at high Zr/Ti ratio.

II. Conclusions

The microstructure of 7.9/70/30 in PLZT transparent ferroelectric ceramics has been studied by using the HREM and SAED techniques and the following experimental results have been obtained.

(1) In the cubic α-phase of PLZT grains exist a certain number of orientated polar micro-regions (micro-domains). The fringe-shaped micro-regions (50—300 Å) shown in the HREM microphotograph are caused by lattice-overlapping of the orthorhombic micro-domains and the cubic α-phase matrix.

(2) The $2\times d_{111}$ superlattice along the $\langle 111\rangle$-direction in 7.9/70/30 PLZT is the result of gliding or rotation due to the self-structure regulation on the (111)-plane in the presence of point defects.

References

[1] Wang, P. C. et al., *Ferroelectrics Letters*, **4**(1985), 1: 47.
[2] Yao Xi et al., *J. Appl. Phys.*, **54**(1983) 6: 3399.
[3] 李承恩、殷之文，硅酸盐学报，**10**(1982)，1: 9.
[4] Hirsch, P. et al., *Electron Microscopy of Thin Crystals*, New York, 1977.
[5] Keve, E. T. et al., *J. Appl, Phys.*, **46**(1975), 2: 810.
[6] 殷之文，新型无机材料，**10**(1982)，3: 39.
[7] Michel, C. et al., *Solid State Commun.*, **1**(1969), 1865.
[8] Yin, Z. W. et al., in *Proc. 6th IEEE International Symposium on Application of Ferroelectrics*, 1986, 139.
[9] 宋祥云、温树林，化学学报，**43**(1985)，3: 282.
[10] 魏宗英，中国科学院上海硅酸盐研究所硕士论文，1981年.